VARIATIONS IN HYDROTHERMAL FLUID CHARACTERISTICS THROUGH TIME AT THE SANTA RITA PORPHYRY COPPER DEPOSIT, NEW MEXICO

by

Theodore James Reynolds

A Thesis Submitted to the Faculty of the

DEPARTMENT OF GEOSCIENCES

In Partial Fulfillment of the Requirements
For the Degree of

MASTER OF SCIENCE

In the Graduate College

THE UNIVERSITY OF ARIZONA

1 9 8 0

STATEMENT BY AUTHOR

This thesis has been submitted in partial fulfillment of requirements for an advanced degree at The University of Arizona and is deposited in the University Library to be made available to borrowers under rules of the Library.

Brief quotations from this thesis are allowable without special permission, provided that accurate acknowledgment of source is made. Requests for permission for extended quotation from or reproduction of this manuscript in whole or in part may be granted by the head of the major department or the Dean of the Graduate College when in his judgment the proposed use of the material is in the interests of scholarship. In all other instances, however, permission must be obtained from the author.

SIGNED: T. James Reynolds

APPROVAL BY THESIS DIRECTOR

This thesis has been approved on the date shown below:

R E Beane

R. E. BEANE
Assistant Professor of Geosciences

10/31/80

Date

ACKNOWLEDGMENTS

The author expresses deepest personal gratitude to Dr. Richard E. Beane, who suggested and directed this research. Sincere appreciation is extended to the following individuals who gave generously of valuable time and patiently assisted in various aspects of this study: Dr. John W. Anthony, Dr. Dennis K. Bird, Robert J. Bodnar, Philip M. Giudice, Frederick M. Haynes, Lawrence C. Johnson, Fleetwood R. Koutz, Daniel J. Lynch, Gregory E. McNew, Dr. Denis L. Norton, Richard K. Preece, Jodi A. Rushing, Francis X. Sousa, Thomas M. Teska, Dr. Spencer R. Titley, Dr. Krishna Seshan, Valerie A. Walker, and William H. Wilkinson. Elizabeth Y. Anthony deserves acknowledgment and special thanks for establishing the semiquantitative method for daughter mineral identification.

This project could not have been completed without permission from Kennecott Copper Corporation or without the kind, generous assistance afforded by Paul Novotny, acting geologist at Santa Rita. Financial support was provided by U. S. National Science Foundation grant EAR-7713642-A01.

TABLE OF CONTENTS

TABLE OF CONTENTS--Continued

LIST OF ILLUSTRATIONS

LIST OF TABLES

ABSTRACT

A fluid inclusion study was designed to trace through time the variations of thermal and gross chemical characteristics of hydrothermal fluids responsible for a specific sequence of alteration-mineralization assemblages at the Santa Rita porphyry copper deposit. Results of over 1,700 fluid inclusion measurements indicate the earliest fluid was a high-temperature (>775°C), hypersaline (about 16-34 molal NaCl ± KCl eq.) brine associated with a barren quartz + orthoclase + biotite + apatite vein. This was followed by a cooler (about 260-500°C) but still highly saline (about 10-20 molal NaCl eq.) fluid associated with a quartz + orthoclase + biotite vein assemblage, which evolved to the coolest (about 240-400°C) high salinity (about 8-16 molal NaCl eq.) solutions associated with quartz + orthoclase deposition in the Whim Hill breccia pipe and characterized by much lower Na/K atomic ratios (about 1.0) than the other groups of high-salinity fluids (about 2.8). In addition to halite, sylvite, and anhydrite; chalcopyrite, magnetite, hematite, potassium feldspar, and mica (muscovite?) have been tentatively identified as daughter products in all generations of hypersaline fluid inclusions using scanning electron microscopy and observable physical properties. A later, lower temperature (260-360°C), low-salinity (<3 molal NaCl eq.) fluid is associated with two alteration assemblages: a quartz + sericite + pyrite assemblage dominant in zones peripheral to chlorite + orthoclase + sulfides + clay assemblages which bear the hypogene copper mineralization at the Santa Rita deposit.

CHAPTER I

INTRODUCTION

Formation of porphyry copper deposits may involve two fluids of different origins. During crystallization in shallow crustal environments, some hydrous magmas become saturated and consequently exsolve water, forming a separate fluid phase. Waters indigenous to the host rocks circulate due to thermal perturbations caused by cooling plutons. Substantial evidence suggests that these magmatic and meteoric fluids may have occupied important roles at different times during the alteration and mineralization history of porphyry copper deposits.

Mathematical models of fluid flow through fractured, permeable plutons indicate that the source regions of the earliest hydrothermal fluids are endogenous, and that later fluids are largely derived from surrounding host rocks (Norton, 1978, in press). Interpretations of stable isotope characteristics of alteration minerals from several porphyry copper deposits (Sheppard, Nielsen, and Taylor, 1969, 1971; Sheppard and Gustafson, 1976) support the results of the mathematical simulations. These workers identify an early fluid derived from magma or equilibrated with igneous rock at magmatic temperatures as being responsible for potassic alteration and mineralization, and correlate phyllic alteration with later influx of cooler meteoric waters derived from adjacent wall rocks. Fluid inclusion studies consistently demonstrate that two fluids, distinguished by contrasting salinities, took

part in the development of alteration and mineralization of these deposits (Roedder, 1971; Nash, 1976). Results of these fluid inclusion investigations, however, do not offer unambiguous evidence pertaining to the origins of the high and moderately saline fluids.

The primary concerns of this investigation are to establish the thermal and gross chemical characteristics of hydrothermal fluids from a porphyry copper deposit, to trace the variations of these characteristics through time, and to correlate fluid types with specific alteration-mineralization assemblages. The Santa Rita porphyry copper deposit was chosen for study because the potassic and phyllic alteration assemblages at the deposit had already been attributed to magmatic and meteoric processes respectively (Sheppard et al., 1971). In this study characteristics of the fluids associated with the alteration types were determined by studying fluid inclusions in quartz which is an integral part of specific assemblages of alteration minerals. Vein and breccia samples containing abundant fluid inclusions were analyzed by petrographic, isotopic, electron microprobe, and fluid inclusion methods. Distinctive qualities of magmatic fluids were sought from early veins thought to have formed at near-magmatic temperatures, based on isotope studies (Sheppard et al., 1971), and from the Whim Hill breccia pipe which Norton and Cathles (1973) attributed to processes related to magmatic crystallization. Solutions with a significant meteoric component (Sheppard et al., 1971) were characterized by study of fluid inclusions in a late quartz + sericite + pyrite vein. Techniques developed by

Preece and Beane (in preparation) and Bodnar and Beane (in press) were employed to monitor changes of fluid properties through time.

CHAPTER II

SUMMARY OF GEOLOGIC RELATIONS

The Santa Rita porphyry copper deposit is located in the Central Mining District of southwestern New Mexico (Figure 1). Hernon, Jones, and Moore (1953) and Jones, Hernon, and Moore (1967) provide detailed information regarding the geologic setting of the Santa Rita Quadrangle. Comprehensive reports on the geology of the Santa Rita stock and the associated mineralization and alteration include those of Kerr et al. (1950), Rose and Baltosser (1966), and Nielsen (1968).

General Geology

In the vicinity of the Santa Rita Quadrangle, a relatively thin (1.2km) sequence of gently dipping, undeformed Paleozoic and Mesozoic sedimentary rocks blanketed a Proterozoic crystalline basement complex in Late Cretaceous time. Limestones, often dolomitic or siliceous with shaly horizons, comprise most of the Paleozoic section which is terminated by redbeds. The Cretaceous units are largely sandstones and shales which rest conformably on quartzite. The Precambrian basement rocks include a variety of granitic rocks, gneisses, quartzites, micaceous schists, and greenstones.

Igneous activity commenced in Late Cretaceous time with the intrusion of quartz diorite sills and laccoliths. The Santa Rita stock intruded the concordant plutons and sedimentary country rocks at about 60 m.y. b.p. (McDowell, 1971); quartz monzonite porphyry and latite

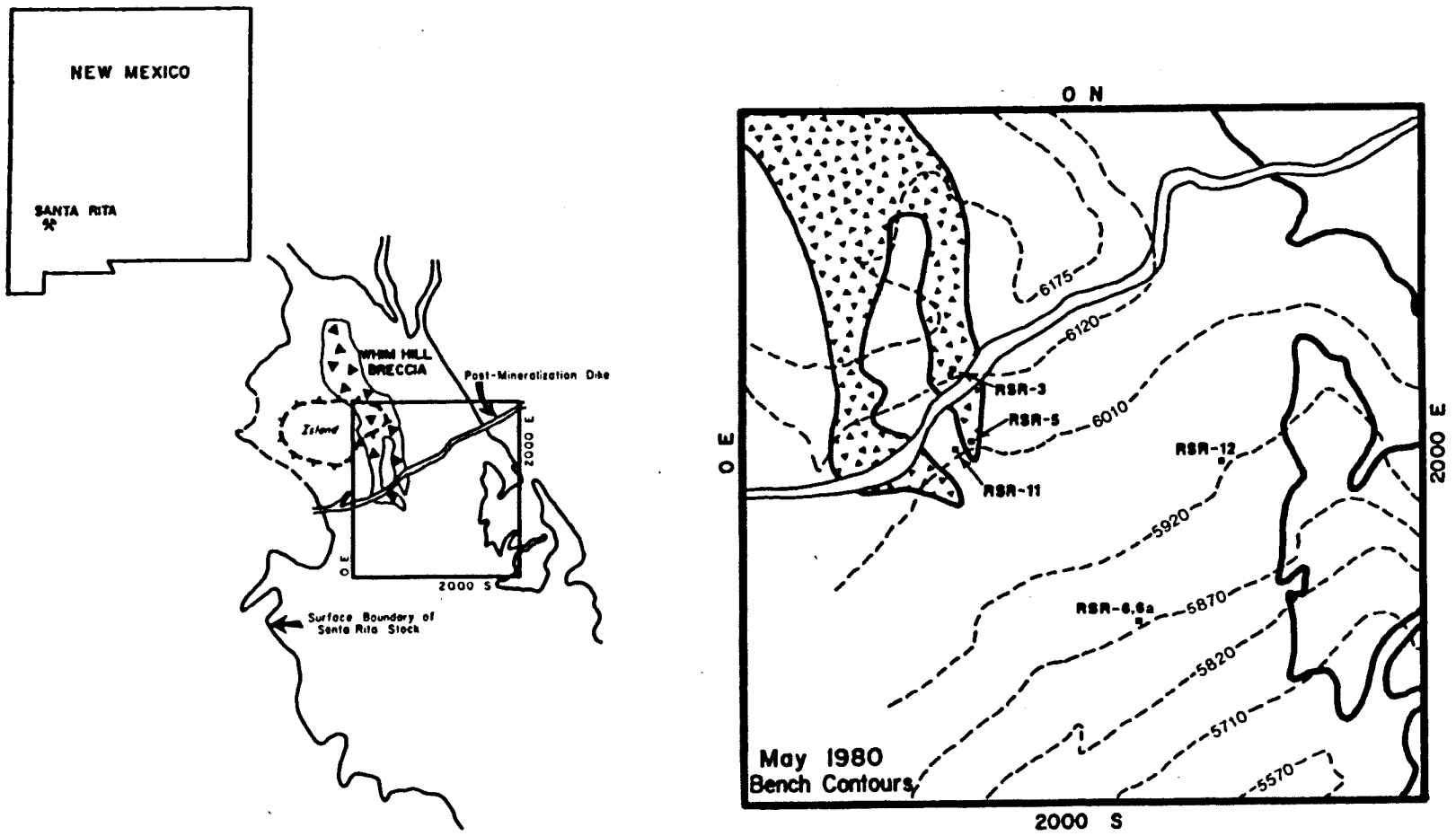

Figure 1. Study Area and Sample Locations. -- Geology after Rose and Baltosser (1966) and Norton and Cathles (1973).

porphyry dikes were then emplaced in the stock and surrounding wall rocks. There followed an extended period of erosion which was terminated by outpourings of rhyolitic and andesitic pyroclastics and flows in mid-Tertiary time.

The ore and associated alteration minerals at Santa Rita are localized in and adjacent to the stock which is transitional in composition between granodiorite and quartz monzonite. Ore-grade copper mineralization in the stock and surrounding wall rocks is the result of supergene enrichment of low-grade primary copper sulfides concentrated along closely spaced fractures. Higher-grade hypogene magnetite-chalcopyrite-pyrite replacement ore bodies are distributed about the margins of the intrusion in calcareous units of Paleozoic age.

Zoning of Hypogene Alteration and Mineralization

Previous studies of hydrothermal alteration at Santa Rita have demonstrated that both gangue and sulfide minerals are distributed in pronounced zones with diffuse boundaries roughly related to the shape of the stock. In central regions of the biotite granodiorite porphyry, alteration is characterized by abundant secondary orthoclase commonly associated with secondary biotite. Here, sulfide mineralization is minimal to nonexistent.

Zones exhibiting destructive alteration of feldspars and biotite, and increasing sulfide content surround the central region of the stock. Biotite is frequently chloritized and orthoclase is stable where clays replace plagioclase; however, both biotite and chlorite are

replaced by sericite in the quartz-sericite zone which occurs on the margins of the stock and in the non-calcareous country rocks. From the low-grade central region toward the margins of the stock, chalcopyrite increases in abundance until reaching a maximum (0.4-1.0 weight percent of the rock) in areas where chlorite, orthoclase, and clay are present. Pyrite content also increases outward from the core, and is most abundant in the peripheral quartz-sericite zone (4-8 weight percent of the rock). The ratio of pyrite to chalcopyrite in the zones of richest hypogene copper mineralization is as low as 3:1, but toward the margins of the stock rapidly increases to 40:1 as quartz, sericite, and pyrite become the dominant alteration phases.

Paragenesis of Hypogene Alteration and Mineralization

Inasmuch as gangue and sulfide minerals occur in veins and in the adjacent wall rock, paragenetic relations among the distinctive alteration assemblages are explicitly defined by the crosscutting relationships among the veins. The paragenetic relationships (Figure 2) provide the framework for establishing the temporal variations in hydrothermal fluid characteristics.

Barren Vitreous Quartz Veins

The earliest generation of veins at Santa Rita are filled with vitreous gray quartz often accompanied by orthoclase or biotite and less commonly apatite. Nielsen (1968) reported that some of these vitreous quartz veins contained molybdenite and chalcopyrite. However, detailed petrographic studies of specimens collected for this investigation led

Figure 2. Paragenetic Sequence of Alteration-mineralization Assemblages. -- v = vein-filling minerals, w = wall rock alteration associated with vein-filling mineralogy, osf = void-filling minerals, fa = breccia fragment alteration. Parentheses denote presence of minerals of ambiguous paragenesis.

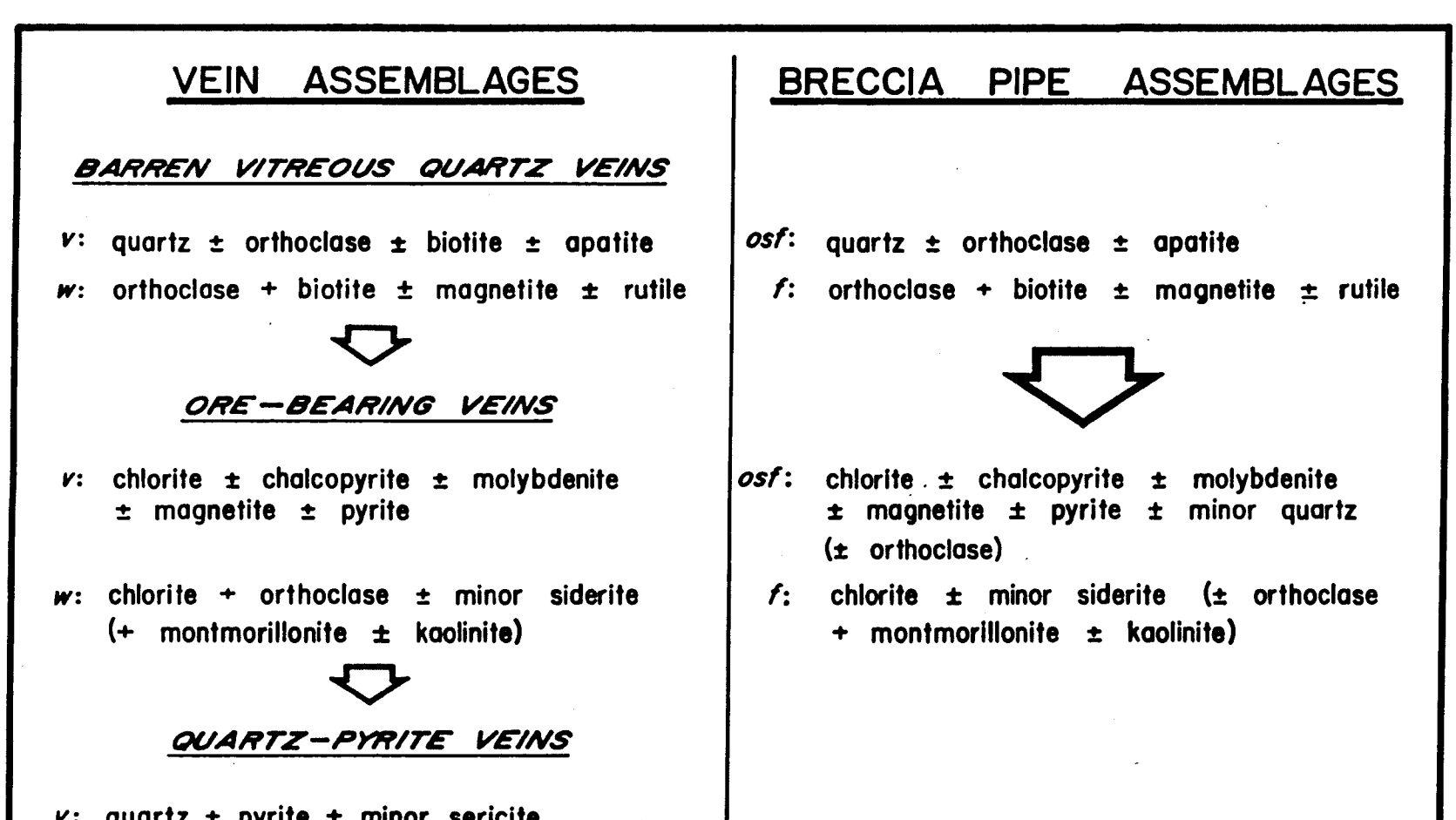

Figure 2. Paragenetic Sequence of Alteration-mineralization Assemblages.

to the conclusion that only reopened veins of this group contained sulfides, as previously concluded by Kerr et al. (1950). In the igneous wall rocks near these veins, secondary biotite replaces original biotite and hornblende, secondary orthoclase floods the groundmass and may replace plagioclase phenocrysts, and rutile and magnetite grains are commonly disseminated near mafic minerals.

The barren quartz veins and the associated wall rock alteration are considered to have formed during the final stages of consolidation of the Santa Rita pluton. Randomly oriented and sometimes folded veins of this type are particularly abundant in the granodiorite intrusion, although a few of these veins occur in the sedimentary and quartz diorite porphyry country rocks. In addition, the vitreous quartz veins predate features considered to be of late magmatic origin: 1) Leroy (1954) described a "hornblende dike", lacking vitreous quartz veins but containing later vein types, which traversed granodiorite porphyry transected by abundant vitreous quartz veins; and 2) the Whim Hill breccia pipe postulated to be of magmatic origin (Norton and Cathles, 1973) contains clasts with terminated vitreous gray quartz veins.

Ore-bearing Veins

Next in the sequence of vein formation is a group of veins that provide the bulk of the hypogene copper mineralization. These are normally thin (less than 3mm) fractures which are filled with any combination of the minerals chalcopyrite, pyrite, molybdenite, and magnetite, and which invariably have associated chlorite. Nielsen (1968) reported pale-green and pale-brown biotite along these veins, but microprobe

analyses of mica minerals during this study demonstrated that chlorite is the stable phase. R. L. Nielsen (personal communication, 1979) confirmed that the chlorite could have been misidentified previously. Siderite is common to the assemblage, and orthoclase, which often forms vein selvages, is always a stable phase. Quartz, if present, is a very minor constituent. Where these veins are present, wall rock plagioclase phenocrysts are replaced to varying degrees by montmorillonite and kaolinite. These chlorite-bearing fractures cut and offset the earlier, barren, vitreous gray quartz veins.

Quartz-pyrite Veins

Veins consisting of quartz + pyrite + minor sericite ± minor chlorite, having well-developed envelopes of pervasive quartz + sericite (fine-grained $2M_1$ muscovite) and minor pyrite, crosscut all other groups of veins in the Santa Rita deposit and are most abundant at the periphery of the stock. Earlier quartz, orthoclase, biotite, montmorillonite, kaolinite, chlorite, and plagioclase are altered to quartz + sericite + pyrite in the vicinity of these late veins.

Whim Hill Breccia Pipe Assemblages

The Whim Hill breccia is an elliptical body (500 x 100m) located in the northern, central regions of the Santa Rita stock, which gradually narrows until it bottoms out about 65m below the upper exposures within the pit (Figure 1). Some of the breccia is composed of angular blocks with coarse, euhedral quartz, orthoclase, apatite, and pyrite crystals occupying portions of the interstitial spaces, whereas other

parts are composed of well-rounded fragments cemented by a porous "rock-flour" matrix. Based on paragenetic relationships among silicate and sulfide minerals filling open space in the Whim Hill breccia pipe (Figure 2) and on microscopic examination of fluid inclusions enclosed in quartz, two mineral assemblages are distinguishable: an early quartz + orthoclase ± apatite assemblage was succeeded by one identical to that of the chlorite-bearing mineralized veins, but which was accompanied by minor amounts of contemporaneous quartz which nucleated and grew on the earlier quartz crystals.

The formation of the breccia pipe post-dates at least some of the structural episodes during which vitreous gray quartz veins were deposited as is evident from the fact that veins of this type are contained within breccia fragments. Aplite dikes less than 5cm thick with mineralogies and textures closely resembling that of the granodiorite porphyry groundmass intrude the breccia, demonstrating that igneous activity continued after breccia formation (Kerr et al., 1950). The thin, chlorite-bearing, mineralized fractures common in unbrecciated biotite granodiorite are not found to cut breccia clasts; however, late replacement and open-space filling in the Whim Hill breccia pipe consist of the same minerals that compose the mineralized veins (Figure 2), indicating that brecciation preceded formation of the ore-bearing fractures.

CHAPTER III

METHOD OF STUDY

Hand specimens were collected from south-facing benches across the "island" between the North and South pits of the Santa Rita deposit. At the time of collection, mining operations had not significantly altered the geometry of the island since the early 1970's. Slabbed surfaces of about 200 samples were studied to corroborate vein and associated wall rock alteration assemblages, and the crosscutting relationships reported in previous studies (Kerr et al., 1950; Nielsen, 1968). Six samples containing a representative cross section of vein and alteration assemblages were selected for detailed petrographic, isotopic, microprobe, and/or fluid inclusion studies (Figure 1). To focus on the thermochemical variations of the hydrothermal fluids through time, the samples to be studied in detail were chosen from a restricted area to eliminate potential spatial variations. Previous studies of hand specimens from the same or nearby locations have been reported by Jacobs (1976), Jacobs and Parry (1979), and Sheppard et al. (1971).

Fluid Inclusion Techniques

Classification of Fluid Inclusions

In this study fluid inclusions were classified by a scheme described by Nash (1976) based on the phases observable in inclusions at

room temperature. An inclusion containing a liquid occupying greater than about 50 volume percent, plus a smaller vapor bubble is referred to as a Type I inclusion. A Type II inclusion contains fluid plus a vapor bubble which occupies more than about 50 volume percent of the inclusion and homogenizes by filling to the vapor phase. Some of these vapor-rich inclusions contain birefringent or opaque daughter phases which do not dissolve upon heating. Type III fluid inclusions contain, in addition to liquid and vapor phases, a daughter mineral identified as halite based on optical characteristics, behavior upon heating, and electron microprobe analyses. Numerous other daughter minerals were often present as well. Some could be tentatively identified using observable physical properties (i.e., shape, color, relief, birefringence, and magnetism), but others required electron microprobe analysis. Non-opaque daughter minerals in the Type III inclusions dissolved below 550°C. Carbon dioxide occurring as a separate phase was not observed in any fluid inclusions from the Santa Rita samples.

Fluid inclusions were also classified as primary, secondary, or pseudosecondary (Roedder, 1979) in the cases where the relative time of trapping by the enclosing mineral could be determined. Quartz observed during this study had been repeatedly fractured as is evident from the abundant planes of fluid inclusions in single specimens. In most instances, the preponderance of these randomly oriented planes prevented determination of whether or not a given inclusion under observation was along a fracture (secondary or pseudosecondary in origin) or was trapped during crystal growth (primary in origin). Nevertheless, copious

fluid inclusion temperature and salinity data permit correlation of groups of inclusions with various alteration and mineralization assemblages. In sections of euhedral quartz crystals cut perpendicular to the c-crystallographic axis, lateral growth zones were observed to be defined by linear arrays of fluid inclusions and bands of chlorite + sulfides oriented parallel to crystal faces (Figure 3). These inclusions are either oblong with smooth surfaces or are of highly irregular shape, and were judged to be of primary origin where crosscutting secondary planes were absent.

Size of Fluid Inclusions

The quartz specimens from Santa Rita contained fluid inclusions ranging in average diameter from less than 1μm to greater than 100μm. Only inclusions with diameters between 3 and 30μm were subjected to heating tests, and only inclusions with average diameters greater than 10μm were subjected to freezing tests. The vast majority of inclusions studied had diameters ranging between 10 and 20μm.

Equipment

Temperatures of phase changes in fluid inclusions were measured with a chromel-alumel thermocouple attached to a Doric Digital Trendicator model 410A during heating and freezing tests using two different dual-purpose heating/freezing stages. A stage previously described by Preece and Beane (in preparation) could be used at temperatures up to 500°C and another "high-temperature stage" of similar design constructed during this study was capable of attaining temperatures up to 800°C.

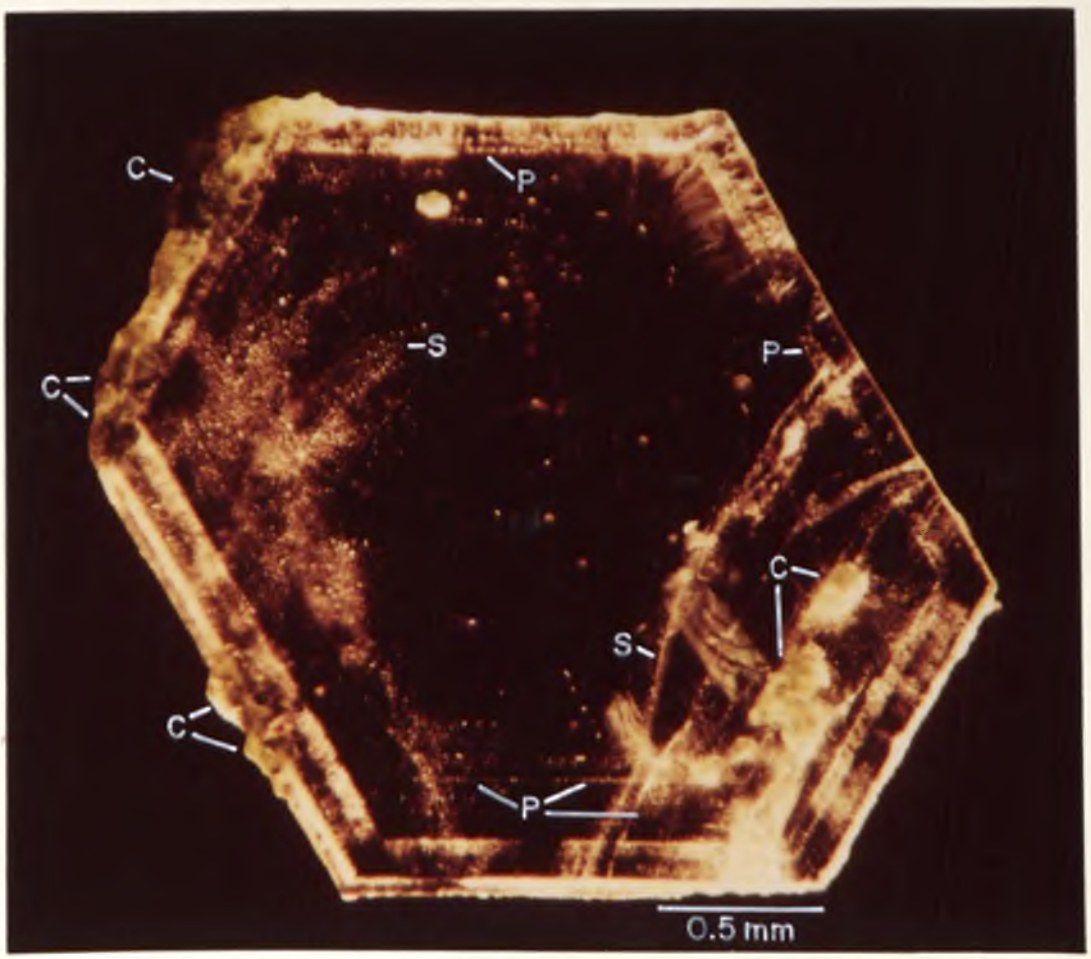

Figure 3. Photomicrograph of a Cross Section of a Quartz Crystal. -- Sample is from the Whim Hill breccia pipe (RSR-5). View is perpendicular to the c-crystallographic axis. Growth zones are defined by linear trains or groups of fluid inclusions shown as tiny white specks. P = train of primary inclusions; S = secondary plane of inclusions; C = greenish chlorite rosettes in outer growth zones.

Both systems were calibrated using melting point standards and were found to be accurate within ±5°C below 500°C. The high-temperature stage required N_2 gas circulation to smooth thermal gradients at temperatures exceeding 500°C, and measured temperatures were found to be accurate within ±10°C upon numerous calibration experiments at 651 and 776°C. The accuracy of measurements between -25 and 0°C is conservatively estimated at ±1.0°C based on numerous calibration runs throughout the course of study at -25.2, -9.6, and 0.0°C. The precision and reproducibility (Bodnar and Beane, in press) were generally much smaller than the measurement accuracy at the calibration temperatures. However, the accuracy and precision of actual temperature measurements of phase changes in fluid inclusions contain additional uncertainties attributable to optical distortions (a function of temperature), the rate of heating during a phase change, and the small size of fluid inclusions.

Procedure

Sections of vein quartz and euhedral quartz crystals which were cut perpendicular to the c-crystallographic axis were polished on each side to thicknesses ranging from about 100-500μm and then sliced to rectangles roughly 2-3mm on a side with a wire saw. Fluid inclusions suitable for heating and/or freezing tests were mapped in detail at low magnification to determine their relationships to the total population of inclusions present in the sample and were then observed at high magnification to determine optical properties of phases in the inclusions at room temperature. All freezing tests were completed prior to heating runs. Each thin slab was subjected to a single sequence of heating runs

designed to determine the homogenization temperature of low-temperature inclusions before subjecting them to higher temperatures. Each run in a sequence achieved a slightly higher temperature (about 10°C) than the previous run. This technique ensured that the entire thermochemical history of fluids recorded by the inclusions was determined. Temperature measurements of phase changes were recorded for about 5-10 fluid inclusions per thin slab.

Homogenization temperatures of fluid inclusions correspond to temperatures of disappearance of the vapor bubble or dissolution of halite, whichever is higher. Salinities were determined either by freezing point depression of Type I inclusions (Potter, Clynne, and Brown, 1978), or halite and sylvite dissolution in Type III inclusions (Keevil, 1942; Roedder, 1971; Potter, Babcock, and Brown, 1977). For a large number of the Type III inclusions, homogenization proceeded by halite dissolution rather than vapor bubble disappearance. Previous studies have suggested that this is not a result of kinetic effects (Bodnar and Beane, in press) as suggested by some researchers (Chivas and Wilkins, 1977; Eastoe, 1978). Experimental solubility data for the system NaCl-H_2O is at vapor saturation, so the salinities determined for Type III inclusions homogenizing by halite dissolution are approximate values only. However, Roedder and Bodnar (1980) indicate that the pressure dependence of NaCl solubility is low at pressures below 1kbar.

Microprobe Techniques

The chemical composition of minerals was determined by electron microprobe analyses performed with an ARL Scanning Electron Microprobe

Quantometer (SEMQ) equipped with a Tracor-Northern automation system for reduction of data. Bence-Albee corrections (Bence and Albee, 1968; Albee and Ray, 1970) were applied to all analyses. Identification of daughter minerals in hypersaline fluid inclusions was aided by use of the SEMQ. A small chip of quartz was split, carbon or gold coated, and mounted for "visual searches" in the scanning mode. Once a daughter mineral was located, it was analyzed for 200 seconds. Energy-dispersive spectral analyses were employed to determine the chemical compositions. The SUPER ML program which incorporates ZAF correction factors was used to convert peak intensities to values of elemental weight percent (Wodke and Schamber, 1976). The precision of this method is limited by the geometry of the inclusion and enclosed daughter mineral. For large (greater than 3μm), well-formed daughter minerals, the precision is within a few weight percent relative. The accuracy (6-8 weight percent relative) is based on comparison of known compositions of materials with analyses of the same reference materials using the SUPER ML program. An expanded discussion of the determination of precision and accuracy is presented by Anthony, Reynolds, and Beane (in preparation). Once analyzed, the quartz chip was transferred to a Super IIIA International Scientific Instruments scanning electron microscope where daughter minerals were photographed.

Isotope Techniques

Oxygen isotopic composition of quartz, orthoclase, biotite, and chlorite from several samples provided a basis for comparison of the results of this study with those of an investigation of veins collected

from Santa Rita previously proposed to have formed from magmatic solutions (Sheppard et al., 1971). Minerals were separated by hand and heavy liquid methods. O^{18}/O^{16} ratios were determined by Professor H. P. Taylor of the California Institute of Technology employing methods similar to those described in Sheppard et al. (1969) and Sheppard and Taylor (1974).

In some cases, temperatures computed from oxygen isotope partitioning between minerals were compared to fluid inclusion data. Temperatures were obtained using the oxygen isotope fractionation data for the quartz-H_2O and feldspar-H_2O systems of Bottinga and Javoy (1973) and the chlorite-H_2O system of Wenner and Taylor (1971).

Presentation of Data

For each of the three main alteration assemblages documented at the Santa Rita porphyry copper deposit, compositional and isotopic data of the minerals, in addition to fluid inclusion data from associated quartz, are presented in Chapters IV and V. Only representative microprobe analyses are tabulated. All isotope data are reported relative to the SMOW standard in the usual δ (per mil) notation. Homogenization temperatures and salinities are shown separately in histogram form, and plots of homogenization temperature versus salinity portray data for which both measurements were obtained from single inclusions. The homogenization temperatures reported are the actual measured values. Salinities are presented as equivalent NaCl molalities when determined either by freezing point depression of Type I inclusions or by halite dissolution of Type III inclusions. For inclusions which contained both halite

and sylvite as daughter products, salinities are plotted as NaCl + KCl equivalent molalities. Compositions of these halite + sylvite-bearing inclusions are interpreted using the NaCl-KCl-H_2O phase diagram given by Roedder (1971).

CHAPTER IV

RESULTS OF ANALYSIS OF EARLY ORTHOCLASE + BIOTITE-STABLE ALTERATION

Vein Samples

Detailed studies of the early quartz + orthoclase + biotite alteration assemblages were conducted on two samples of biotite granodiorite porphyry that contained vitreous quartz veining. The vein in sample RSR-12 contained intergrown, medium- to coarse-grained, anhedral, vitreous gray quartz; coarse laths of biotite with interlayered chlorite exceeding 50%; coarse, euhedral apatite crystals; and minor orthoclase. Sample RSR-6 was very similar in vein mineralogy except that apatite was absent, and chlorite was not detected by petrographic, x-ray, or microprobe techniques. Neither vein contained sulfides, and each displayed selvages of orthoclase.

Mineral Compositions

Microprobe analyses indicate that alteration orthoclase--partially disordered according to D. Bird and J. Trembly (personal communication, 1980)--is virtually identical in composition to unaltered wall rock orthoclase (Or_{90-96}). The vein-filling biotite differs markedly from fresh igneous phenocrysts (Table 1), corresponding with observations previously reported by Jacobs and Parry (1979). As illustrated in Figure 4, molar Mg/(Mg + Fe) of biotites decreases progressively from vein biotite (greater than .68) to igneous biotite phenocrysts (less

Table 1. Representative Microprobe Analyses of Ferromagnesian Silicates. -- amph = amphibole, biot = biotite, ← = after, chl = chlorite.

WEIGHT % OXIDES

		SiO_2	Al_2O_3	FeO	MgO	MnO	TiO_2	CaO	N_2O	K_2O	Total
"fresh" rock	1 amph	49.86	5.49	12.05	16.29	0.65	0.85	11.85	0.93	0.59	98.55
	2 biot	35.36	14.24	16.59	14.78	0.27	4.96	0.00	0.32	8.96	95.47
	3 biot (←amph)	36.73	13.47	16.39	16.01	0.28	4.33	0.06	0.06	8.36	95.68
RSR-12	4 vein biot	37.11	14.93	13.78	19.25	0.10	1.63	0.06	0.20	7.87	94.94
	5 chl (←vein biot)	28.97	18.13	17.10	23.35	0.18	0.23	0.08	0.05	0.49	88.59
RSR-6	6 vein biot	38.40	14.05	12.76	18.84	0.03	3.30	0.03	0.24	9.49	97.14
	7 wall rk biot	37.36	15.29	14.17	16.12	0.15	4.37	0.02	0.22	9.62	97.32
RSR-11	8 wall rk biot	36.59	14.67	15.66	14.74	0.09	4.86	0.01	0.28	8.85	95.76
	9 chl (←w.r. biot)	26.96	19.68	20.28	19.24	0.29	0.06	0.03	0.01	0.02	86.58
	10 vein chl	26.74	20.77	22.16	18.68	0.60	0.01	0.01	0.00	0.09	89.05
RSR-3	11 clast biot	36.72	14.38	17.57	13.27	0.16	4.25	0.01	0.26	9.00	95.62
	12 clast chl(←biot)	26.63	18.75	22.12	16.97	1.09	0.00	0.18	1.52	0.10	87.35
	13 open sp. chl	27.50	19.26	22.90	18.11	1.39	0.02	0.04	0.08	0.09	89.38
RSR-5	14 clast chl(←biot)	27.68	19.50	17.30	19.98	2.67	0.01	0.08	0.07	0.06	87.35
	15 open sp. chl	28.47	19.20	18.74	20.17	1.73	0.00	0.07	0.17	0.06	88.62

ATOMIC PROPORTIONS

	Si	Al^{IV}	Al^{VI}	Ti	Fe(II)	Mn	Mg	Ca	Na	K	# oxygens	$\frac{Mg}{Mg+Fe}$
1	7.19	0.81	0.12	0.09	1.45	0.08	3.50	1.83	0.26	0.11	23	.707
2	5.35	2.54	0.00	0.56	2.10	0.03	3.33	0.00	0.09	1.73	22	.613
3	5.50	2.38	0.00	0.49	2.05	0.03	3.57	0.01	0.02	1.60	22	.635
4	5.49	2.51	0.09	0.18	1.71	0.01	4.25	0.01	0.06	1.49	22	.713
5	2.14	1.86	0.28	0.02	1.43	0.02	3.48	0.01	0.01	0.06	14	.709
6	5.57	2.40	0.00	0.36	1.55	0.00	4.07	0.00	0.07	1.76	22	.724
7	5.45	2.55	0.08	0.48	1.73	0.02	3.51	0.00	0.06	1.79	22	.670
8	5.46	2.54	0.04	0.55	1.95	0.01	3.28	0.00	0.08	1.68	22	.627
9	2.80	1.20	1.21	0.00	1.76	0.03	2.98	0.00	0.00	0.00	14	.629
10	2.73	1.27	1.23	0.00	1.89	0.05	2.84	0.00	0.00	0.01	14	.600
11	5.54	2.46	0.10	0.48	2.22	0.02	2.98	0.00	0.08	1.73	22	.573
12	2.81	1.19	1.14	0.00	1.95	0.10	2.67	0.02	0.31	0.01	14	.578
13	2.82	1.18	1.15	0.00	1.96	0.12	2.77	0.00	0.01	0.01	14	.586
14	2.84	1.16	1.20	0.00	1.48	0.23	3.05	0.01	0.01	0.01	14	.673
15	2.88	1.12	1.17	0.00	1.59	0.15	3.04	0.01	0.03	0.01	14	.657

than .63), with alteration biotite intermediate in composition. Microprobe analyses of biotite along traverses perpendicular to several veins of similar alteration mineralogy reveal compositional variations comparable to those in Figure 4, suggesting that biotite compositions are related to proximity to fractures as well as to mode of origin. In the quartz + orthoclase + biotite + apatite vein, the Mg/Mg + Fe mole ratio of replacement chlorite is approximately the same as the remaining biotite (Table 1).

Homogenization Temperatures and Salinities

Results of heating and freezing tests on 752 fluid inclusions from vitreous quartz of the two veins are depicted in Figure 5A to H. The upper histogram in Figure 5A shows two groups of fluid inclusions from the quartz + orthoclase + biotite + apatite vein which homogenize by disappearance of the vapor bubble (L+V → L). The first group consists of hypersaline (Figure 5B) inclusions homogenizing at or above 775°C. The possibility that these high homogenization temperatures result from leakage, necking-down, or mixed-phase entrapment has been discredited for several reasons. The high-temperature fluid inclusions are prevalent throughout the vein, and in several instances the salt and vapor phases enclosed by inclusions within a single plane reacted simultaneously to changes in temperature during a heating run. Furthermore, once the hiatus of homogenization temperatures between about 500 and 775°C (Figure 5C) became apparent, directed studies were undertaken to locate inclusions homogenizing in this range, yet few were observed. This conspicuous gap is, in itself, evidence opposing leaking and necking of

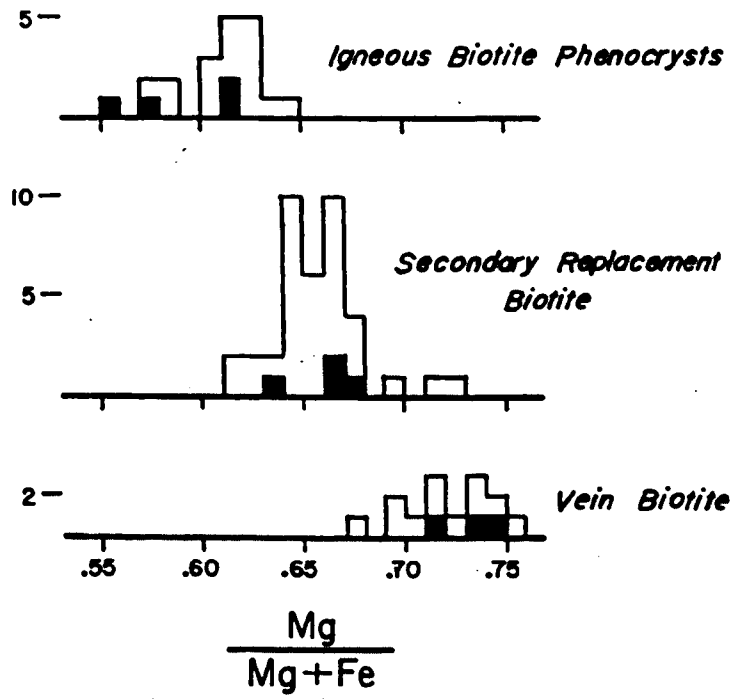

Figure 4. Compositional Variation of Biotite of Contrasting Origin. -- These histograms were constructed with data of this study (solid) and with data selected from Jacobs (1976, Appendix A).

Figure 5. Fluid Inclusion Data of the Early Orthoclase + Biotite-stable Alteration Assemblages. -- Rows contain data from the single sample denoted at the left of a row. Different types of data are displayed in each column to facilitate comparison of data from the three samples. The symbols employed for each column are noted at the base. The scales on the abscissas in the lowest row apply to an entire column.

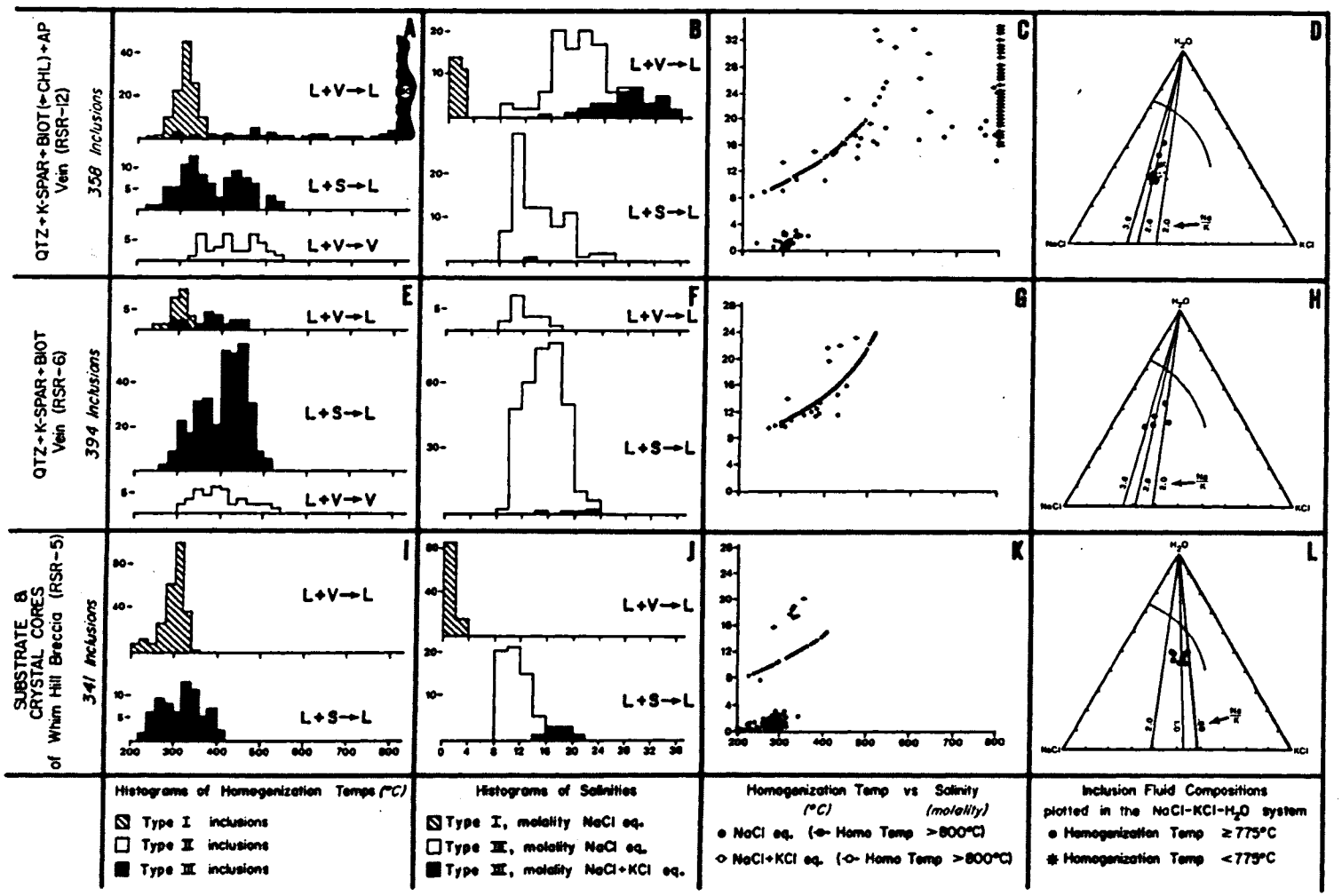

Figure 5. Fluid Inclusion Data of the Early Orthoclase + Biotite-stable Alteration Assemblages.

inclusions or formation by mixed-phase entrapment as viable mechanisms for the formation of these high-temperature inclusions: had these processes occurred, a continuum of homogenization temperatures would have resulted. The second group of inclusions in the upper histogram of Figure 5A homogenized to liquid by vapor bubble disappearance at temperatures in the range 260-360°C and are of low salinity. The middle histogram of Figure 5A shows temperatures at which a third group of inclusions in this vein homogenized to the liquid phase by halite dissolution (L+S → L): these temperatures range from 260-500°C and are bimodally distributed. The lower histogram in Figure 5A demonstrates that Type II, vapor-rich, inclusions homogenize generally in the range 340-520°C, though the precision of homogenization temperature measurements for vapor-rich inclusions is very poor (±25°C).

Figure 5B contains histograms of fluid salinities shown as equivalent chloride molalities determined either by freezing point depression of Type I fluid inclusions or by halite (and sometimes halite + sylvite) dissolution of Type III fluid inclusions. Salinities of the highest temperature group of inclusions range from about 16-34 molal NaCl ± KCl eq. (Figure 5B, upper histogram). The inclusions with the highest salinity (solid area of Figure 5B) contained both halite and sylvite daughter products. The Type I inclusions which homogenized by vapor bubble disappearance have salinities less than 3 molal NaCl eq. (Figure 5B, upper histogram). Salinity values for Type III inclusions homogenizing by halite solution generally range from about 9-20 molal NaCl eq. (Figure 5B, lower histogram). Figure 5C shows homogenization

temperatures and salinities of fluid inclusions in the quartz + orthoclase + biotite + apatite vein for which both properties could be determined. Na/K molar ratios for inclusion fluids of this vein are plotted on the NaCl-KCl-H_2O compositional triangle (Figure 5D) and average about 2.8.

Temperatures and salinities of the fluid inclusions of the quartz + orthoclase + biotite vein (RSR-6) are generally similar to those of the vein described above, as may be seen by comparing Figure 5E to H with Figure 5A to D. The two important differences are: 1) the high-temperature (greater than 775°C), high-salinity group of Type III inclusions were not observed in this sample, and 2) Type I inclusions were only rarely noted. The paucity of Type I, liquid-rich, fluid inclusions in the vein containing fresh biotite (RSR-6) permits a tentative correlation of low-temperature, low-salinity fluids with the chloritization of biotite noted in the quartz + orthoclase + biotite + apatite vein (RSR-12). Additional evidence for this correlation is presented in Chapter V. In vein RSR-6, most inclusions homogenize by halite dissolution at temperatures ranging from 300-480°C (Figure 5E, middle histogram) with a major peak at 400-480°C. This same peak of homogenization temperatures, also by salt dissolution, is present in the quartz + orthoclase + biotite + apatite vein (Figure 5A, middle histogram).

Comparing Figure 5A and E, it appears that the moderate-temperature, high-salinity inclusions of the quartz + orthoclase + biotite vein could have been superposed on the RSR-12 vitreous quartz vein

as secondary inclusions. This possibility, and the fact that the high-temperature, high-salinity group of inclusions is absent in this vein, suggest that formation of the RSR-6 vein post-dated filling of the RSR-12 vein. This argument supports the contention that the high-temperature, high-salinity fluids were some of the earliest to circulate and alter the Santa Rita biotite granodiorite porphyry stock.

In summary, fracturing and filling of some barren vitreous gray quartz veins with the associated orthoclase + biotite alteration commenced at temperatures exceeding 800°C, yet the alteration assemblage was apparently stable in the presence of high-salinity fluids to as low as 260°C. Few inclusions were observed to homogenize between 500 and 775°C in this study (Figure 5C and G).

Daughter Minerals

The high-salinity inclusions typically display a host of daughter minerals which have been tentatively identified based on observable physical properties and on morphology viewed with the scanning electron microscope. Some of the phases observed are documented in Figure 6 and Table 2, and include halite, sylvite, anhydrite, chalcopyrite, magnetite, hematite, potassium feldspar, and mica (muscovite?).

The general chemical character of the hypersaline fluids may be determined from measurements of daughter crystal dimensions and the diameters of roughly spherical host inclusions. A density of 1.0 g/cm^3 (Roedder and Bodnar, 1980, fig. 2) was employed to estimate the minimum concentrations of iron, sulfur, and copper dissolved in a single Type III fluid inclusion (average diameter of about 14μm) containing an

Figure 6. Scanning Electron Photomicrographs of Daughter Minerals Observed in Type III Fluid Inclusions. -- Arrows point to daughter minerals analyzed. Beneath each micrograph is the energy-dispersive waveform of the daughter mineral shown. Major peaks of the elements present in the minerals are labeled. Unlabeled peaks are either gold (from the preparation procedure), silicon (from the surrounding quartz cavity), or other elements (from nearby daughter minerals). All bar scales denote a length of 1 micron. A = halite, B = sylvite, C = anhydrite, D = chalcopyrite, E = magnetite, F = hematite, G = potassium feldspar, H = mica (muscovite?). Stoichiometry of these daughter minerals as determined from semiquantitative microprobe analyses are presented in Table 2.

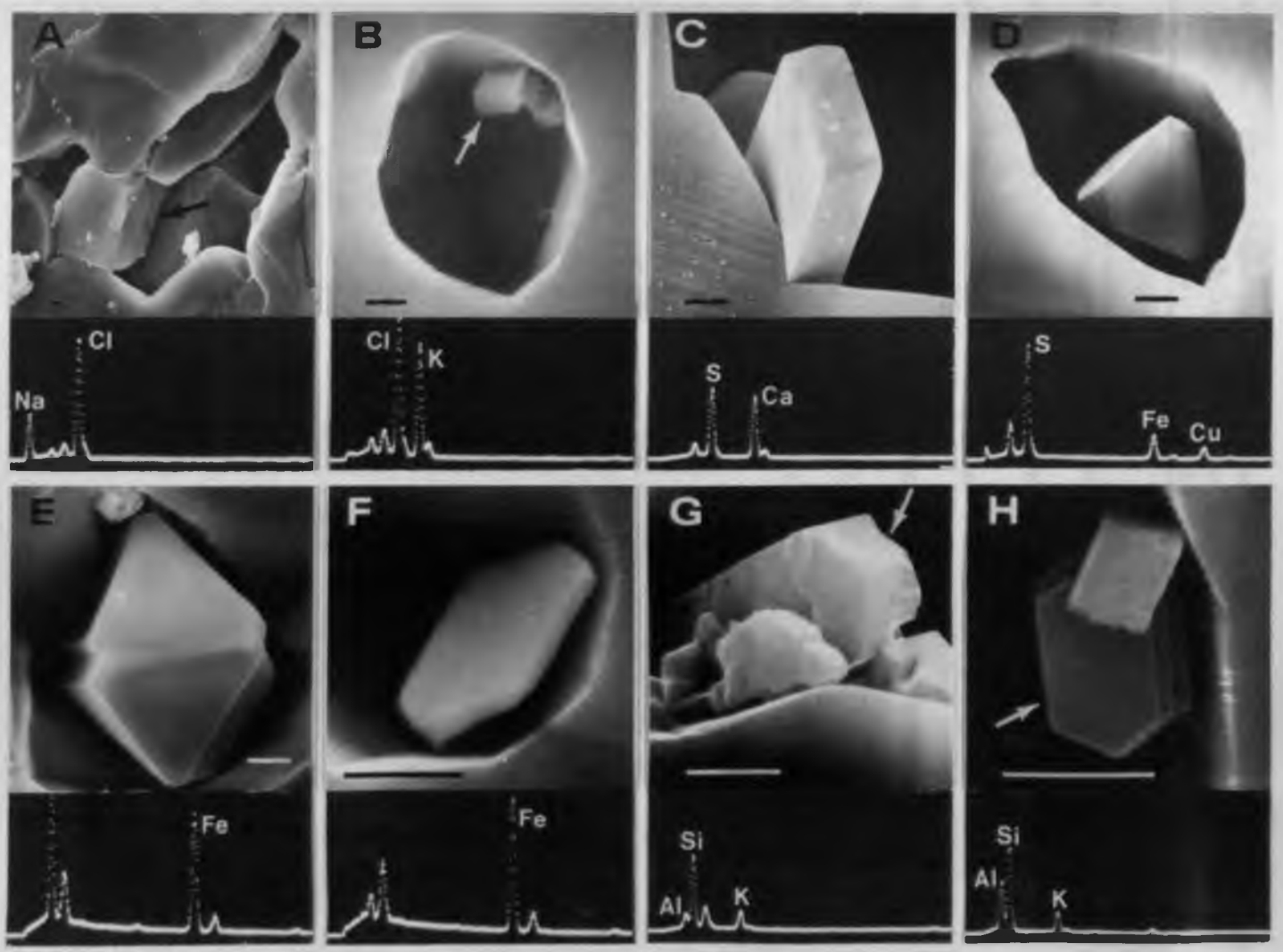

Figure 6. Scanning Electron Photomicrographs of Daughter Minerals Observed in Type III Fluid Inclusions.

Table 2. Stoichiometry of Daughter Minerals. -- Atomic proportions are determined by analysis of the energy-dispersive spectra shown in Figure 6. Analyses by E. Anthony.

MINERAL	ATOMIC PROPORTIONS		
Halite	Na = 0.98	Cl = 1.00	
Sylvite	K = 1.07	Cl = 1.00	
Anhydrite	Ca = 1.08	S = 1.00	
Chalcopyrite	Cu = 1.05	Fe = 1.08	S = 2.00
Potassium feldspar	K = 0.87	Na = 0.16	Al = 1.00
Mica (muscovite?)	K = 1.00	Al^{IV+VI} = 3.16	

average-sized (edge of about 4μm) chalcopyrite daughter mineral: Fe≈7000 ppm, S≈8000 ppm, Cu≈8000 ppm.

Pressure Estimates

In all samples studied from Santa Rita, vapor-rich (Type II) fluid inclusions were always observed in quartz that contained halite-bearing (Type III) inclusions; Type II inclusions never accompanied Type I, liquid-rich, inclusions in the absence of Type III inclusions. In veins RSR-12 and RSR-6, vapor-rich inclusions homogenize in the same temperature range as the Type III inclusions which usually homogenize by halite dissolution (Figure 5A and E, lower histograms). These data suggest that the high-salinity fluids could have coexisted with vapor at some time during the history of the orthoclase + biotite-stable alteration event, although unequivocal evidence for the simultaneous entrapment of Type II and Type III inclusions was not noted. Employing data of Sourirajan and Kennedy (1962), a range of possible minimum pressures that existed during vein filling may be established with knowledge of the homogenization temperatures of the vapor-rich inclusions, and the salinities of the fluids which are interpreted as having undergone boiling. Saturated salt solutions boiling at temperatures between 300 and 525°C indicate pressures ranging from about 65 to 360 bars.

The halite-bearing inclusions homogenizing by vapor bubble disappearance at temperatures exceeding 775°C could require pressures at the time of entrapment of at least 1000 bars by extrapolation of data for the pure NaCl-H_2O system (Sourirajan and Kennedy, 1962). However,

the numerous other constituents dissolved in the solutions could reduce this minimum pressure estimate, perhaps significantly.

Oxygen Isotope Ratios

δO^{18} values of the quartz (8.2‰, RSR-6; 8.3‰, RSR-12) and orthoclase (7.7‰, RSR-6; 7.1‰, RSR-12) correspond closely with phenocrysts and other early vitreous quartz veins from Santa Rita reported previously (Sheppard et al., 1971). Oxygen isotope fractionations between quartz and orthoclase of these veins yielded unreasonably high temperatures (1390°C, RSR-6; 900°C, RSR-12), as did the fractionation between quartz and biotite ($\Delta O^{18}_{q-b} = 1.7$) of sample RSR-6 (Sheppard et al., 1971, fig. 5). This information suggests retrograde isotopic exchange of orthoclase and biotite but not of quartz (Sheppard et al., 1971). Retrograde exchange may be related to the fluids of relatively low temperature which occur in fluid inclusions in quartz from the veins.

Whim Hill Breccia Samples

In samples of Whim Hill breccia, two mineral assemblages (Figure 2) are distinguishable based on studies of paragenetic relationships among silicate and sulfide minerals filling open spaces and microscopic examination of fluid inclusions in three separate modes of occurrence of quartz in this structure. Some breccia clasts are thinly coated with anhedral quartz and orthoclase forming a substrate from which project large euhedral quartz and orthoclase crystals. Quartz crystals cut perpendicular to the c-crystallographic axis exhibited several periods of

growth. These periods were distinguished by linear arrays of fluid inclusions oriented parallel to crystal faces and by inclusions of chlorite and sulfides deposited along crystal faces of the outermost zones (Figure 3). Deposition of early quartz of the substrate and crystal cores clearly preceded deposition of material in the outer growth zones of the quartz crystals. Quartz of the substrate and crystal cores contain abundant Type I, Type II, and Type III fluid inclusions. However, in the later, volumetrically minor (usually less than 10 volume percent of an individual crystal), outer growth zones containing solid inclusions of chlorite and sulfides, only Type I inclusions are present. Furthermore, planes of pseudosecondary halite-bearing inclusions always terminate at the first growth zone containing sulfides and chlorite. These microscopic relationships convincingly demonstrate that hypersaline and vapor-rich inclusion types were trapped during formation of the early quartz substrate and quartz crystal cores contemporaneous with early orthoclase, and are thus considered to be primary with respect to the generation of quartz within which they occur.

Results of heating tests from hand samples RSR-3 and RSR-5 are virtually identical; data of RSR-5 are presented in Figure 5I to L. Primary and pseudosecondary inclusions in the substrate and crystal cores homogenize by halite dissolution (L+S → L) at about 240-400°C (Figure 5I, lower histogram), and salinities in the range 8-16 molal NaCl eq. (Figure 5J, lower histogram). Pseudosecondary vapor-rich inclusions were too small to permit confident determination of homogenization temperatures. Many of the same daughter minerals identified in the

early vitreous gray quartz veins were also noted in these saline inclusions, but Na/K molar ratios (from halite + sylvite-bearing inclusions) differ markedly from the ratios of fluids trapped by the earlier vitreous quartz veins (compare Figure 5D and H with 5L).

These moderate-temperature, hypersaline fluids responsible for early deposition of quartz and orthoclase in the breccia pipe could have been represented as secondary inclusions in earlier-formed veins: there is a crude correspondence of the peaks of homogenization temperatures lower than 400°C in the histograms for inclusions homogenizing by halite disappearance (L+S → L) in Figure 5A, E, and I.

Also present in the substrate and crystal cores of the breccia pipe quartz is a group of secondary Type I inclusions with homogenization temperatures primarily in the range 260-340°C (Figure 5I, upper histogram) and salinities averaging less than 3 molal NaCl eq. (Figure 5J, upper histogram). This group of inclusions is identical (in homogenization temperature distribution) to the group of low-temperature, low-salinity secondary fluid inclusions previously suggested to be the fluids which chloritized the biotite of the early vitreous quartz vein (RSR-12) deposited from high-temperature, hypersaline solutions (Figure 5A). Further support for this correlation is drawn from the fact that these Type I secondary inclusions correlate with the primary fluid inclusions from the outer growth zones of the Whim Hill breccia quartz crystals discussed in Chapter V.

CHAPTER V

RESULTS OF ANALYSIS OF LATE ALTERATION ASSEMBLAGES

Chlorite + Orthoclase + Sulfides + Clay Alteration

Numerous mineralized veins collected from various localities around the "island" at Santa Rita contain combinations of chalcopyrite, pyrite, molybdenite, and magnetite, often bordered by a thin selvage of orthoclase. Chlorite replaces both igneous and alteration biotite in narrow zones paralleling the veins and is itself commonly enclosed or surrounded by sulfides or magnetite in these thin veins. Wall rock plagioclase is invariably replaced by mixtures of montmorillonite and kaolinite. Evidence for coeval deposition of quartz in these veins was lacking. However, identical alteration-mineralization assemblages present in the Whim Hill breccia contain a minor amount of late quartz which coated the euhedral quartz crystals deposited from earlier hypersaline fluids. As microscopic overgrowths of quartz accumulated, chlorite and sulfides were enclosed as solid inclusions, while Type I, liquid-rich, fluid inclusions were trapped. Fluid inclusions aligned in trains or groups parallel to crystal faces (Figure 3) are considered primary in origin and are suitable for characterizing the ore-forming fluids. Secondary and igneous orthoclase which precipitated earlier than the outer growth zones of quartz was stable during the late chlorite + sulfide depositional event in the breccia pipe. Biotite in

the breccia clasts is partially to completely replaced by chlorite, and igneous plagioclase is pervasively altered to montmorillonite and kaolinite.

Mineral Compositions

Microprobe analyses of chlorite and biotite in samples containing veins with chalcopyrite (locality RSR-11) and in breccia samples RSR-3 and RSR-5 reveal that the Mg/(Mg + Fe) mole ratios of precipitated chlorite are comparable to those of biotite in adjacent wall rock or of biotite in breccia clasts (Table 1). In one mineralized vein studied (RSR-11), chlorite intergrown with chalcopyrite showed Mg/(Mg + Fe) mole ratios between .60 and .62 mole fraction clinochlore, and the wall rock biotite and replacement chlorite had Mg/(Mg + Fe) mole ratios of .63 (Table 1). Similar results were obtained from sample RSR-3 (Table 1) which contained abundant chalcopyrite. In Whim Hill breccia sample RSR-5 where chalcopyrite is rare, chlorite which replaced biotite in the clasts, and chlorite which precipitated contemporaneously with pyrite in open spaces displayed molar Mg/(Mg + Fe) ratios of roughly .67 and .66, respectively. The results of these microprobe studies suggest that the composition of chlorite precipitating with sulfides is closely related to the composition of biotite in the adjacent wall rock (or breccia fragments).

Homogenization Temperatures and Salinities

The outer growth zones of the euhedral quartz crystals from the Whim Hill breccia pipe samples contain primary Type I fluid inclusions

which record the thermal and chemical characteristics of fluids associated with the chlorite + orthoclase + sulfide + clay alteration assemblages. These inclusions homogenize at temperatures in the range 260-360°C (Figure 7A). The small size of the primary inclusions (5-10μm) usually prohibited determination of salinity by freezing; nevertheless, salinities less than 1 molal NaCl eq. (Figure 7B) were obtained from 11 successful freezing tests. Similar low-temperature, low-salinity fluids are contained in secondary inclusions in quartz deposited during the early orthoclase + biotite-stable alteration event (compare Figure 7A with Figure 5A and I; Figure 7B with Figure 5B and J; and Figure 7C with Figure 5C and K). These chlorite-stable fluids were probably responsible for the pervasive alteration of hydrothermal vein biotite to chlorite in the RSR-12 vein sample (Figure 5A, Table 1).

Oxygen Isotope Ratios

Oxygen isotope fractionations among possible pairs of the three minerals quartz (δO^{18} = 9.0‰), orthoclase (δO^{18} = 6.1‰), and chlorite (δO^{18} = 0.3‰) from breccia sample RSR-5 yielded temperatures of 305°C (ΔO^{18}_{q-k}), 301°C (ΔO^{18}_{q-c}), and 299°C (ΔO^{18}_{k-c}). These concordant temperatures are in good agreement with the fluid inclusion data for the early quartz + orthoclase breccia pipe assemblage which precipitated from hypersaline fluids at 240-400°C, and with the data for the late chlorite + sulfide assemblages which precipitated from low-salinity fluids at 260-360°C. Inasmuch as pressure variations do not affect isotope partitioning among minerals, the close correlation of results from the separate geothermometric techniques suggests that pressure

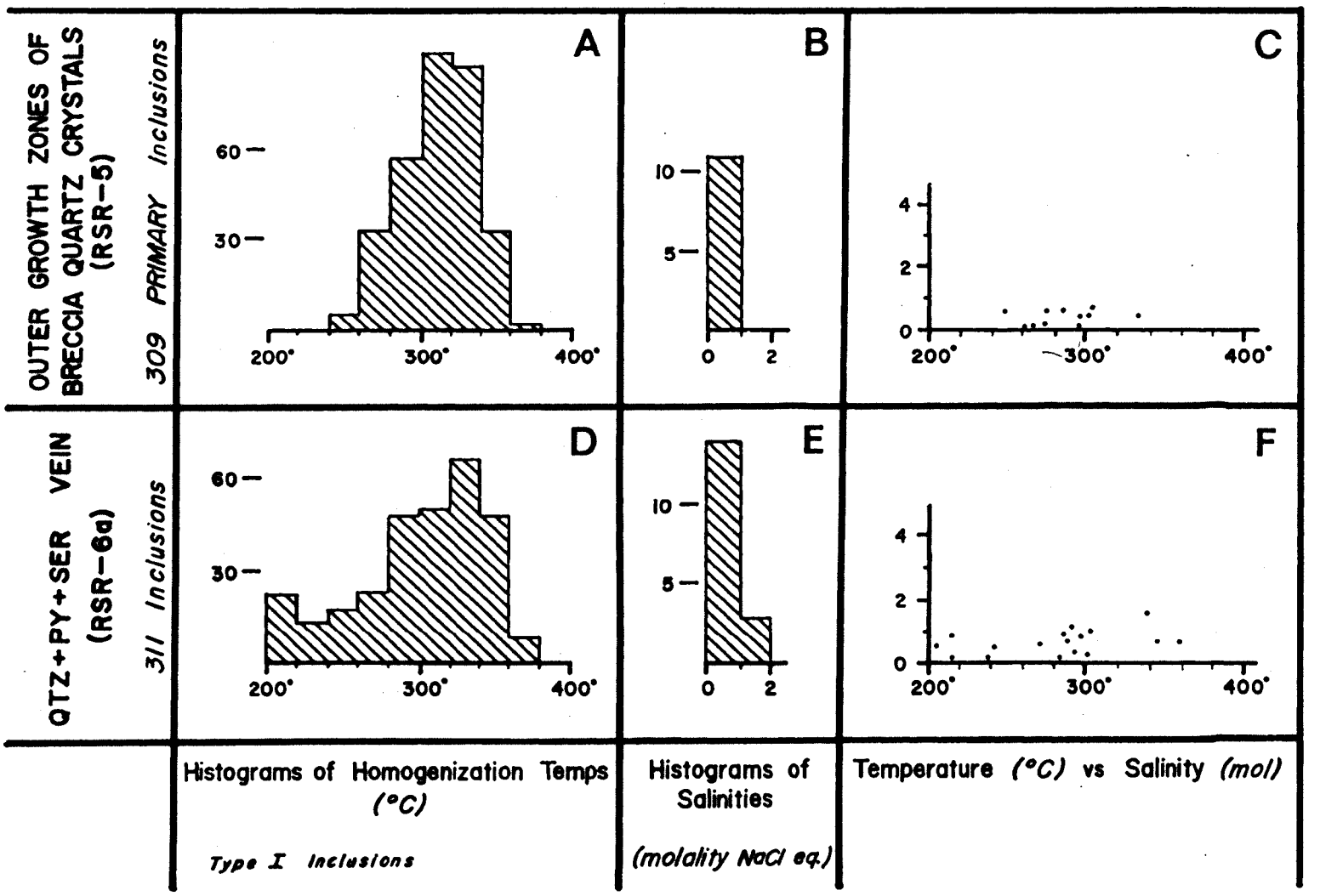

Figure 7. Fluid Inclusion Data of the Late Alteration Assemblages.

corrections to homogenization temperatures of fluid inclusions from the breccia pipe are not significant. In the absence of coexisting vapor-rich inclusions, pressures for the low-salinity fluids over this temperature interval must exceed values for boiling solutions: pressures of boiling, 1.9 molal NaCl solutions at 260 and 360°C are 44 bars (Haas, 1976) and 166 bars (Sourirajan and Kennedy, 1962), respectively. If pressures had been on the order of 400 bars, pressure corrections to these homogenization temperatures would be on the order of +30°C.

Quartz + Sericite + Pyrite Alteration

A single vein from biotite granodiorite porphyry (RSR-6a) exhibiting the quartz + sericite + pyrite alteration was studied to assess the thermal and chemical characteristics of the hydrothermal fluids associated with this alteration type. Only a few very distinctive, nearly vertical, continuous, planar veins of this type occurred at this sample location, but each clearly crosscut all earlier vein assemblages. The sampled vein contained milky-white quartz intergrown with euhedral pyrite plus very minor chlorite, and displayed a well-developed, texturally destructive alteration halo composed largely of quartz, sericite, and pyrite. Only low-salinity Type I fluid inclusions were distinguished in this vein. The peak range of homogenization temperatures (primarily 280-360°C) corresponds closely to that of the primary fluid inclusions in the outer growth zones of the breccia pipe crystals (compare Figure 7A with D). Inclusions greater than 10μm were seldom located, but 17 successful freezing runs yielded salinities not exceeding 1.5 molal NaCl eq. (Figure 7E and F). Thus, the assemblages of chlorite + orthoclase +

sulfides + clay and quartz + sericite + pyrite appear to have formed from hydrothermal solutions of comparable temperatures and salinities (compare Figure 7A, B, and C with Figure 7D, E, and F).

After correcting for original igneous quartz physically inseparable from the quartz + sericite samples, Sheppard et al. (1971) calculated temperatures of 285-380°C for formation of the quartz + sericite assemblage based on oxygen isotope fractionation between these two minerals. This temperature is in good agreement with that obtained from the fluid inclusions studied. Approximations of the minimum pressures obtained during formation of the quartz + sericite + pyrite assemblage should roughly correspond to pressures estimated for the chlorite + orthoclase + sulfides + clay assemblages reported above (44-166 bars), and pressure corrections to fluid inclusion homogenization temperatures are thus probably less than +30°C.

CHAPTER VI

SUMMARY AND DISCUSSION

Based on spatial and temporal relationships among geologic features observed in the field in conjunction with mineralogic, isotopic, and fluid inclusion investigations performed in the laboratory, the thermochemical evolution of the hydrothermal solutions associated with the sequence of alteration-mineralization assemblages at the Santa Rita porphyry copper deposit is summarized as follows:

1) Early, hypersaline (about 8-34 molal NaCl ± KCl eq.) hydrothermal solutions circulated through fractures confined primarily to the Santa Rita stock, and were associated with the early orthoclase + biotite-stable alteration assemblages. Some alteration minerals formed at temperatures in excess of 775°C, but the assemblages remained stable to temperatures as low as about 260°C. Temperatures decreased with concomitant diminution of both the salinities and Na/K atomic ratios (from 2.8 to 1.0) of the fluids. Vapor and liquid could have coexisted at temperatures between 300 and 525°C. These early fluids were complex chloride brines with high concentrations of sodium, potassium, copper, iron, and sulfur, but sulfide minerals were not precipitated in the veins through which they traversed.

2) Later, non-boiling, low-salinity (less than 3 molal NaCl eq.) solutions circulated through newly-formed fractures and older

reopened veins at temperatures primarily 260-360°C, and effected the formation of two distinct alteration assemblages. Moving laterally away from central portions of the stock, predominant alteration changes from chlorite + orthoclase + sulfides + clay assemblages bearing the hypogene copper mineralization to peripheral zones characterized by the quartz + sericite + pyrite assemblage. Though the chlorite + orthoclase + sulfide + clay assemblages precede the quartz + sericite + pyrite assemblage in any given hand sample, coeval development of the two assemblages in separate regions of the geothermal system is not precluded.

The results of the fluid inclusion studies complement the conclusions of previous investigations. Jacobs and Parry (1979) interpreted the compositions of biotite found within the central orthoclase + biotite alteration zone as indicating formation temperatures of 745 ± 20°C and pressures exceeding 1000 bars. Employing the biotite geothermometer of Beane (1974), temperatures estimated for the orthoclase + biotite alteration assemblage range from 360-530°C (Beane, 1974; Jacobs and Parry, 1979). Also, interpretations of stable isotope ratios of early barren vitreous gray quartz veins and associated orthoclase + biotite-stable alteration indicate temperatures in the range 390-500°C (Sheppard et al., 1971). Discordant quartz + orthoclase temperatures were taken to indicate retrograde isotopic exchange probably continuing to temperatures as low as 270°C (Sheppard et al., 1971). Temperatures derived from fluid inclusion analyses of the solutions related to the

chlorite + orthoclase + sulfides + clay assemblages support the results of previous isotopic studies of the montmorillonite and kaolinite (Sheppard et al., 1969) which demonstrated that all of the clay beneath the lower level of detectable chalcocite at Santa Rita and much of the clay within the enriched blanket was hypogene in origin. In addition, the fluid inclusion data from the quartz + sericite + pyrite vein presented here compare well with results of previous isotopic studies which indicated temperatures ranging from 285-380°C with retrograde exchange continuing to 240°C for this alteration assemblage (Sheppard et al., 1971).

The stable isotope and fluid inclusion studies suggest that two fluids of contrasting chemical, thermal, and isotopic character took part in the development of alteration during formation of the Santa Rita porphyry copper deposit. Furthermore, the data support the proposal that at least some of the high-salinity fluids effecting the early orthoclase + biotite-stable alteration were magmatic (that is, of igneous origin or exchanged with igneous rocks at magmatic temperatures). Cooler, low-salinity fluids, suggested by isotope ratios to be of meteoric origin, pervaded the stock as new fractures formed and were associated with the development of the two later alteration-mineralization assemblages.

Evidence for Magmatic Origin of the High-salinity Fluids

As reviewed by Burnham (1979), exsolution of a magmatic aqueous phase is a predictable consequence of igneous melts solidifying in shallow crustal environments. Experimental results indicate that Na/K

atomic ratios of aqueous phases exsolved from a granodioritic magma may vary from 0.3 to 4.0 during the crystallization history (Burnham, 1979). Na/K ratios of the high-temperature brines observed in the course of the present investigation lie within this range (2.0-3.6). The correlation of experimentally determined Na/K ratios with the ratios obtained from fluid inclusion measurements and the fact that some fluids were trapped at temperatures exceeding 775°C is good evidence that the high-temperature, hypersaline (about 16-34 molal NaCl ± KCl eq.) inclusions contained fluids derived from a crystallizing magma.

Burnham (1979) suggests that the high-salinity fluid inclusions found at many porphyry copper deposits result from condensation of a low-salinity, low-density fluid subsequent to its separation from a crystallizing melt. Such an explanation is supported by vapor-rich and hypersaline, liquid-rich inclusions homogenizing between 300 and 500°C in this study, but vapor-rich inclusions are not observed with the high-salinity fluid inclusions homogenizing at magmatic temperatures at Santa Rita.

Hypersaline inclusions that homogenized between 260 and 500°C from the orthoclase + biotite-stable veins exhibited the same variety of daughter minerals as was observed in the high-salinity magmatic inclusions, and Na/K ratios of the two generations of fluid are comparable. The δO^{18} of quartz from the quartz + orthoclase + biotite vein (8.2‰, RSR-6) closely compared with that of the quartz from the quartz + orthoclase + biotite + apatite vein (8.3‰, RSR-12), even though only the latter sample contained the high-temperature, high-salinity group of

inclusions. Therefore, the evidence suggests that these later hypersaline fluid inclusions could be cooler analogues of fluids derived from crystallizing magma.

Though the high-salinity inclusions in the quartz substrate and crystal cores from the Whim Hill breccia samples contained a similar variety of daughter minerals to those of the high-salinity fluid inclusions found in the vitreous gray quartz vein samples, Na/K atomic ratios of the fluids from the breccia samples ranged from 0.9-1.6, averaging 1.0, which is significantly lower than the average ratio of the magmatic solutions (about 2.8). The fluids which circulated through the breccia pipe post-dated those which precipitated orthoclase + biotite in the early barren vitreous quartz veins; therefore, the Na/K data of the breccia pipe fluid inclusions are consistent with experimental results discussed by Burnham (1979) that indicate that the Na/K atomic ratios of magmatic aqueous phases could decrease markedly during the evolution of solidifying magma. The suggestion that these moderate-temperature, high-salinity fluids in the breccia pipe samples are of magmatic origin must remain tentative until more definitive evidence is discovered.

The interpretation that the hypersaline fluids associated with the earliest quartz + orthoclase + biotite-stable alteration assemblages at Santa Rita are of magmatic origin parallels that of previous investigators who based their conclusions on stable isotope studies of these minerals. Sheppard et al. (1971) and Taylor (1974) reported that the δD and δO^{18} values of hydrothermal biotites from several porphyry copper deposits throughout the western Cordillera cluster around values similar

to "normal" igneous biotites and show no variation with latitude, suggesting that the hydrothermal biotites probably formed from fluids of magmatic-hydrothermal origin.

Evidence for Meteoric Origin of the Low-salinity Fluids

Alteration assemblages of magmatic-hydrothermal origin can be distinguished isotopically from assemblages of meteoric-hydrothermal origin only in porphyry systems located in regions where the D/H ratios of the local meteoric waters differed appreciably from the magmatic waters throughout the history of the geothermal systems. Though such D-depleted meteoric fluids were not present during the evolution of the Santa Rita porphyry copper deposit, data from other deposits at more northern latitudes (Butte, Wickes, San Poil, Ima) conclusively demonstrate that meteoric waters must have been an important constituent of the hydrothermal solutions from which the hypogene clays and sericites formed (Taylor, 1979). Also, the δD values of these minerals from Santa Rita and other porphyry copper deposits distributed throughout the western Cordillera define a systematic pattern of progressive D depletion in clays and sericites from the southerly to the northerly deposits. The fact that the hypogene sericites and clays from all of these deposits are O^{18}-depleted is compelling evidence that meteoric fluids contributed significantly to the development of the late alteration-mineralization assemblages (Sheppard et al., 1969, 1971; Taylor, 1974). Thus, by inference, meteoric fluids probably comprised a major portion of the

solutions involved in the formation of the clay-stable and sericite-stable assemblages at Santa Rita.

Chalcopyrite Mineralization

A multitude of complexly related chemical and physical parameters may influence the stability of chalcopyrite. Several mechanisms for chalcopyrite deposition are not supported by the data collected in this study. The fact that vapor-rich fluid inclusions are never associated with the chlorite + orthoclase + sulfides + clay assemblages convincingly eliminates concentration-by-boiling as a process involved in the deposition of chalcopyrite at Santa Rita. The distinct gap in salinities exhibited by the fluid inclusions from Santa Rita argues against the suggestion that chalcopyrite deposition resulted from cooling and dilution of magmatic solutions rich in copper, iron, and sulfur upon mixing with meteoric water. If mixing of the two fluids had occurred, then a gap would not be expected to exist in fluid salinities. Thus, the hiatus in the fluid inclusion data is probably the result of a discrete change in fluid properties rather than continuous evolution.

The conversion of iron-bearing silicates to chlorite may have been an important reaction effecting deposition of chalcopyrite at Santa Rita. Results of the microprobe analyses of this study showed that pyrite was the dominant sulfide in the presence of chloritized, high-magnesian biotite (Mg/Mg + Fe≈0.66-0.71), whereas chalcopyrite was commonly abundant in the vicinity of chloritized high-ferroan biotite (Mg/Mg + Fe≈0.57-0.63). Though the ultimate sources of the metals and

sulfur are currently unknown, results of this study conducted at the Santa Rita porphyry copper deposit indicate that in a given small volume of rock, chalcopyrite deposition is temporally intermediate between early potassic alteration and later phyllic alteration, and may be closely related to chemical reactions occurring between hydrothermal solutions of dominantly meteoric origin and either igneous minerals or minerals produced at earlier stages of alteration by magmatic fluids.

REFERENCES

Albee, A. L. and Ray, L., 1970, Correction factors for electron probe microanalysis of silicates, oxides, carbonates, phosphates, and sulfates: Anal. Chem., v. 42, p. 1409-1414.

Anthony, E. Y., Reynolds, T. J., and Beane, R. E., in preparation, SEM/EDS study of daughter minerals in fluid inclusions from Santa Rita, New Mexico: University of Arizona.

Beane, R. E., 1974, Biotite stability in the porphyry copper environment: Econ. Geol., v. 69, p. 241-256.

Bence, A. E. and Albee, A. L., 1968, Empirical correction factors for the electron microanalysis of silicates and oxides: Jour. Geol., v. 76, p. 382-403.

Bird, D. K. and Trembly, J. A., 1980, Personal communication regarding research in progress: Department of Geosciences, University of Arizona.

Bodnar, R. J. and Beane, R. E., in press, Temporal and spatial variations in hydrothermal fluid characteristics during vein filling in pre-ore cover overlying deeply-buried porphyry copper mineralization at Red Mountain, Arizona: Econ. Geol.

Bottinga, Y. and Javoy, M., 1973, Comments on oxygen isotope geothermometry: Earth Planet. Sci. Lett., v. 20, p. 250-265.

Burnham, C. W., 1979, Magmas and hydrothermal fluids, in Geochemistry of Hydrothermal Ore Deposits, Barnes, H. L. (ed.), Second Edition: John Wiley and Sons, Inc., New York, p. 71-136.

Chivas, A. R. and Wilkins, R.W.T., 1977, Fluid inclusion studies in relation to hydrothermal alteration and mineralization at the Koloula porphyry copper prospect, Guadalcanal: Econ. Geol., v. 72, p. 153-169.

Eastoe, C. J., 1978, A fluid inclusion study of the Panguna porphyry copper deposit, Bougainville, Papua New Guinea: Econ. Geol., v. 73, p. 721-748.

Haas, J. L., Jr., 1976, Physical properties of the coexisting phases and the thermochemical properties of the H_2O component in boiling NaCl solutions: U. S. Geol. Survey Bull. 1421-A, 73 p.

Hernon, R. M., Jones, W. R., and Moore, S. L., 1953, Some geological features of the Santa Rita quadrangle: New Mexico Geol. Soc., Guidebook to Fourth Field Conference, p. 117-129.

Jacobs, D. C., 1976, Geochemistry of biotite in the Santa Rita and Hanover-Fierro stocks, Central Mining District, Grant County, New Mexico: Ph.D. dissertation, University of Utah, Salt Lake City, Utah, 212 p.

Jacobs, D. C. and Parry, W. T., 1979, Geochemistry of biotite in the Santa Rita porphyry copper deposit, New Mexico: Econ. Geol., v. 74, p. 860-887.

Jones, W. R., Hernon, R. M., and Moore, S. L., 1967, General geology of Santa Rita quadrangle, Grant County, New Mexico: U. S. Geol. Survey Prof. Paper 555, 144 p.

Keevil, N. B., 1942, Vapor pressures of aqueous solutions at high temperatures: Jour. Am. Chem. Soc., v. 64, p. 841-850.

Kerr, P. G., Kulp, J. L., Patterson, C. M., and Wright, R. J., 1950, Hydrothermal alteration at Santa Rita, New Mexico: Geol. Soc. America Bull., v. 61, p. 275-348.

Leroy, P. G., 1954, Correlation of copper mineralization with hydrothermal alteration in the Santa Rita porphyry copper deposit, New Mexico: Geol. Soc. America Bull., v. 65, p. 739-768.

McDowell, F. W., 1971, K-Ar ages of igneous rocks from the western United States: Isochron/West, v. 2, p. 1-16.

Nash, J. T., 1976, Fluid inclusion petrology-data from porphyry copper deposits and applications to exploration: U. S. Geol. Survey Prof. Paper 907-D, 16 p.

Nielsen, R. L., 1968, Hypogene texture and mineral zoning in a copper-bearing granodiorite porphyry stock, Santa Rita, New Mexico: Econ. Geol., v. 63, p. 37-50.

_____, 1979, Personal communication at G.S.A. convention in San Diego, California, while employed by The Anaconda Copper Company, Denver, Colorado.

Norton, D., 1978, Sourcelines, sourceregions, and pathlines for fluids in hydrothermal systems related to cooling plutons: Econ. Geol., v. 73, p. 21-28.

Norton, D., in press, Transport processes related to copper-bearing porphyritic plutons: fluid and heat transport in pluton environments typical of the southeastern Arizona copper porphyry province, in Advances in the Geology of the Porphyry Copper Deposits of Southwestern North America, Titley, S. R. (ed.): University of Arizona Press.

Norton, D. and Cathles, L. M., 1973, Breccia pipes-products of exsolved vapor from magmas: Econ. Geol., v. 68, p. 540-546.

Potter, R. W., Jr., Babcock, R. S., and Brown, D. L., 1977, A new method for determining the solubility of salts in aqueous solutions at elevated temperatures: Jour. Res. U. S. Geol. Survey, v. 5, p. 389-395.

Potter, R. W., Jr., Clynne, M. A., and Brown, D. L., 1978, Freezing point depression of aqueous sodium chloride solutions: Econ. Geol., v. 73, p. 284-285.

Preece, R. K. and Beane, R. E., in preparation, Contrasting evolutions of hydrothermal alteration in quartz monzonite and quartz diorite at the Sierrita porphyry copper deposit, Arizona: University of Arizona.

Roedder, E., 1971, Fluid inclusion studies on the porphyry type deposits at Bingham, Utah, Butte, Montana, and Climax, Colorado: Econ. Geol., v. 66, p. 98-120.

_____, 1979, Fluid inclusions as samples of ore fluids, in Geochemistry of Hydrothermal Ore Deposits, Barnes, H. L. (ed.), Second Edition: John Wiley and Sons, Inc., New York, p. 688-693.

Roedder, E. and Bodnar, R. J., 1980, Geologic pressure determinations from fluid inclusion studies: Ann. Rev. Earth Planet. Sci., v. 8, p. 263-301.

Rose, A. W. and Baltosser, W. W., 1966, The porphyry copper deposit at Santa Rita, New Mexico, in Geology of the Porphyry Copper Deposits, Southwestern North America, Titley, S. R. and Hicks, C. L. (eds.): University of Arizona Press, Tucson, Arizona, p. 205-220.

Sheppard, S.M.F. and Gustafson, L. B., 1976, Oxygen and hydrogen isotopes in the porphyry copper deposit at El Salvador, Chile: Econ. Geol., v. 71, p. 1549-1559.

Sheppard, S.M.F., Nielsen, R. L., and Taylor, H. P., Jr., 1969, Oxygen and hydrogen isotope ratios of clay minerals from porphyry copper deposits: Econ. Geol., v. 64, p. 755-777.

Sheppard, S.M.F., Nielsen, R. L., and Taylor, H. P., Jr., 1971, Hydrogen and oxygen isotope ratios in minerals from porphyry copper deposits: Econ. Geol., v. 66, p. 515-542.

Sheppard, S.M.F. and Taylor, H. P., Jr., 1974, Hydrogen and oxygen isotope evidence for the origins of water in the Boulder batholith and the Butte ore deposits, Montana: Econ. Geol., v. 69, p. 926-946.

Sourirajan, S. and Kennedy, G. C., 1962, The system H_2O-NaCl at elevated temperatures and pressures: Am. Jour. Sci., v. 260, p. 115-141.

Taylor, H. P., Jr., 1974, The application of oxygen and hydrogen isotope studies to problems of hydrothermal alteration and ore deposition: Econ. Geol., v. 69, p. 843-883.

_____, 1979, Oxygen and hydrogen isotope relationships in hydrothermal mineral deposits, in Geochemistry of Hydrothermal Ore Deposits, Barnes, H. L. (ed.), Second Edition: John Wiley and Sons, Inc., New York, p. 236-277.

Wenner, D. B. and Taylor, H. P., Jr., 1971, Temperatures of serpentinization of ultramafic rocks based on O^{18}/O^{16} fractionation between coexisting serpentine and magnetite: Contrib. Mineral. Petrol., v. 32, p. 165-185.

Wodke, N. F. and Schamber, F., 1976, SUPER ML: operation and program description: version 1: Tracor Northern Publication NS-885, 49 p.